Three-dimensional velocity field for blood flow using the power-law viscosity function

FERNANDO CARAPAU
Universidade de Évora
Departamento de Matemática and CIMA-UE
Rua Romão Ramalho, 59, 7001-671 Évora
PORTUGAL
flc@u vora.pt

RICARDO CONCEICAO
Universidade de Évora
Renewable Energies Chair and IES-UE
Palácio Vimioso, 7002-554 Évora
PORTUGAL
rfc@uevora.pt

Abstract: The three-dimensional model associated with blood fl w where viscosity depends on shear-rate, such power-law type dependence, is a complex model to study in terms of computational optimization, which in many relevant situations becomes infeasible. In order to simplify the three-dimensional model and as an alternative to classic one-dimensional models, we will use the Cosserat theory related with flui dynamics to approximate the velocity fiel and thus obtain a one-dimensional system consisting of an ordinary differential equation depending only on time and on a single spatial variable, the fl w axis. From this reduce system, we obtain the unsteady equation for the mean pressure gradient depending on the volume fl w rate, Womersley number and the fl w index over a finit section of the tube geometry. Attention is focused on some numerical simulations for constant and non-constant mean pressure gradient using a Runge-Kutta method and on the analysis of perturbed fl ws. In particular, given a specifi data we can get information about the volume fl w rate and consequently we can illustrate the three-dimensional velocity fiel on the constant circular cross-section of the tube. Moreover, we compare the three-dimensional exact solution for steady volume fl w rate with the corresponding one-dimensional solution obtained by the Cosserat theory.

Key–Words: Cosserat theory, blood fl w, shear-thinning fluid one-dimensional model, power-law model, volume fl w rate, mean pressure gradient.

1 Introduction

The study of blood fl w in the cardiovascular system has always fascinated scientists, particularly mathematicians, physicists, biologists, chemists and engineers. Also, the fascination for the subject demonstrated by the artists is relevant, where the anatomical drawings of the genius of Leonardo Da Vinci are highlighted. The earliest records of this study date back to 3500 BC in the Egyptian period, later becoming somewhat more elaborate in the Greek, Roman and Islamic periods. After that, in the seventeenth century, the European scientist William Harvey was the firs to present an accurate explanation on blood fl w in the cardiovascular system in his work entitled *Exercitatio anatomica de motu cordis et sanguinis in animalibus*, see [1]. In our days, we know that blood is a very complex flui and the mathematical modelling of blood fl w is a difficul and challenging problem. The human circulatory system is a closed network of vessels carrying blood. Blood is a suspension of particles (mainly red blood cells, white blood cells and platelets) in a flui called plasma and the vessels can be regarded as hollow tubes with different scales. Generally, blood may be considered as a homogeneous fluid In large arteries, blood may exhibit a standard behavior of a Newtonian flui and the wall may be considered elastic (or mildly viscoelastic). The small arteries are characterized by a strong branching and may, in general, be considered rigid. Here, blood exhibits non-Newtonian phenomenon due to shear-thinning viscosity (see e.g. Chien et al. [2, 3]) and viscoelasticity effects, mainly stress relaxation and normal stress difference effects, see Thurston [4]. Moreover, when we consider arterioles, capillaries and venules, the microstructure and rheological behavior of blood cannot be avoided since the dimension of the blood particles are now of the same order of that of the vessel. Here, phenomena like aggregation and deformability of red blood cells have great influ ence on the rheological behavior of blood, especially on its viscosity at low shear-rates, and blood must be considered as a shear-thinning and viscoelastic fluid see e.g. Chien et al. [2, 3] and, Baskurt and Meiselman [5]. Modelling blood fl w through the human circulatory system is certainly a very complex problem. Among others, we refer to the following difficul ties: the complex geometry of the vessels, complex rheological behavior of blood, pulsatility of the fl w fiel and consequently pulsatility of the walls, complex inelastic permeable walls, different deformability of the red cells at different shear-rates and the lack of boundary data to close the corresponding mathematical models. As a consequence of all these complex aspects related to the three-dimensional model to study blow fl w the idea in this article is to present an alternative theory to reduce the three-dimensional model to a one-dimensional model. In historical point of view, Euler in the eighteenth century was the firs to introduce one-dimensional models to study blood fl w in the human circulatory system, see [6]. The classical one-dimensional models governing equations can be obtained by firs integrating the incompressibility condition and the axial component of linear momentum for the blood fl w fiel over the circular cross-section of the tube and introducing some assumptions related with the nonlinear convective acceleration and the viscous dissipation terms. These closure approximations are typically based on assuming a purely axial fl w with a fi ed dependence on axial variables, for more detail, see e.g. [7, 8, 9]. As an alternative, we consider one-dimensional models obtained by the Cosserat theory (also called director theory) associated with flui dynamics (see Caulk and Naghdi [10]), where the only approximation in account is related with the three-dimensional velocity field The reduce model is obtained by integrating the linear momentum equation over the circular cross-section of the tube, taking a velocity fiel approximation provided by the Cosserat theory. This procedure yields a one-dimensional system, depending only on time and a single spatial variable. The velocity fiel approximation satisfie exactly both the incompressibility condition and the kinematic boundary condition. A detailed discussion about this director theory can be found in the work of Naghdi et al. [11, 12]. The relevance of using a director theory is not in regarding it as an approximation to three-dimensional equations, but rather in their use as independent theories to predict some of the main properties of the three-dimensional problems. Advantages of the director theory include: the theory incorporates all components of the linear momentum; it is a hierarchical theory, making it possible to increase the accuracy of the model; there is no need for closure approximations; the fl w fiel is not assumed to be uni-directional; invariance under superposed rigid body motions is satisfie at each order and the wall shear stress enters directly in the formulation as a dependent variable. Here we are interested in studying the initial boundary value problem for incompressible homogeneous power-law fluid to model blood fl w in a straight circular rigid and impermeable walled vessel with constant radius. Using this director theory, we can intend to predict the main properties of a three-dimensional given problem, where the flui three-dimensional velocity fiel [1]

$$\boldsymbol{\vartheta} = \boldsymbol{\vartheta}(\boldsymbol{x}, t) = \vartheta_i \boldsymbol{e}_i$$

is approximated by[2] (see [10]):

$$\boldsymbol{\vartheta} = \boldsymbol{v} + \sum_{N=1}^{k} x_{\alpha_1} \dots x_{\alpha_N} \boldsymbol{W}_{\alpha_1 \dots \alpha_N}, \tag{1}$$

with

$$\boldsymbol{v} = v_i(z,t)\boldsymbol{e}_i, \quad \boldsymbol{W}_{\alpha_1 \dots \alpha_N} = W^i_{\alpha_1 \dots \alpha_N}(z,t)\boldsymbol{e}_i. \tag{2}$$

This velocity fiel approximation (1) satisfie both the incompressibility condition and the kinematic boundary condition exactly. In condition (1), $\boldsymbol{v}$ represents the velocity along the axis of symmetry z at time t, $x_{\alpha_1} \dots x_{\alpha_N}$ are the polynomial weighting functions with order k (this number identifie the order of the hierarchical theory and is related to the number of directors), the vectors $\boldsymbol{W}_{\alpha_1 \dots \alpha_N}$ are the director velocities which are symmetric with respect to their indices and $\boldsymbol{e}_i$ are the associated unit basis vectors. The selection of such weighting functions represents an important aspect of the formulation of our problem. A good choice of these weighting functions can reduce the complexity of the system of ordinary differential equations in the director formulation of the theory. This choice should be consistent with the hierarchical structure of the basic theory so that the equations for each level of the hierarchy include the equations of all lower orders. The vectors $\boldsymbol{W}_{\alpha_1 \dots \alpha_N}$ are related to physical features of the fluid Using this approach with nine directors (i.e., $k = 3$ at condition (1)) and integrating the equations for the conservation of linear momentum over a circular cross-section of the flui domain, we obtain the unsteady equation for the mean pressure gradient depending on the volume fl w rate, Womersley number and the fl w index over a finit section of the tube geometry. Attention is focused on some numerical simulations for constant and non-constant mean pressure gradient using a Runge-Kutta method and on the analysis of perturbed fl ws. In particular, given a specifi data we can get information about the volume fl w rate and consequently we can illustrate the three-dimensional velocity fiel on

[1] Let $\boldsymbol{x} = (x_1, x_2, x_3)$ be the rectangular space cartesian coordinates (for convenience we set $x_3 = z$) and t is the time variable.

[2] In the sequel, latin indices subscript take the values $1, 2, 3$; greek indices subscript $1, 2$, and the usual summation convention is employed over a repeated index.

the constant circular cross-section of the tube. Moreover, we compare the three-dimensional exact solution for steady volume fl w rate with the corresponding one-dimensional solution obtained by the Cosserat theory. Recently, a director theory approach for modeling blood fl w in the arterial system, as an alternative to the classical one-dimensional models, has been introduced by Sequeira et al. [13, 14]. At work [13] blood is considered as a Newtonian flui and in the work [14], blood is considered as a non-Newtonian fluid where viscosity depends on the shear-rate. This article is a review work based on [14] where new results will be presented. This new results are concerning to the behavior of the three-dimensional velocity fiel in the circular cross-section of a tube with constant radius along the axis of the fl w and on the analysis of perturbed fl ws.

2 Governing equations

Let us model blood as a homogeneous shear-thinning flui moving within a straight and impermeable rigid tube of constant circular cross-section, the vessel domain Ω, see Figure 1. The boundary $\partial\Omega$ is composed

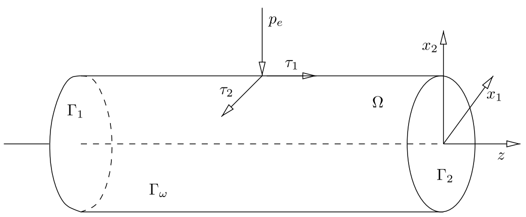

Figure 1: Fluid domain Ω with normal and tangential components of the surface traction vector p_e and τ_1, τ_2 with constant circular cross-section along the axis of symmetry z.

by the proximal cross-section Γ_1, by the distal cross-section Γ_2 and by the lateral wall of the tube Γ_w, define by the constant scalar function[3] ϕ, which is related to the circular cross-section of the tube by the following relationship

$$\phi^2 = x_1^2 + x_2^2. \tag{3}$$

For our haemodynamics problem, the equations of axisymmetric motion, stating the conservation of linear momentum without body forces and mass are given, in $\Omega \times (0, T)$, by

$$\begin{cases} \rho\Big(\dfrac{\partial \boldsymbol{\vartheta}}{\partial t} + \boldsymbol{\vartheta}\cdot\nabla\boldsymbol{\vartheta}\Big) = \nabla\cdot\boldsymbol{T}, \\ \nabla\cdot\boldsymbol{\vartheta} = 0, \\ \boldsymbol{T} = -p\boldsymbol{I} + \mu\big(|\dot{\gamma}|\big)\boldsymbol{A}_1, \quad \boldsymbol{t}_w = \boldsymbol{T}\cdot\boldsymbol{\eta}, \end{cases} \tag{4}$$

with the initial condition

$$\boldsymbol{\vartheta}(\boldsymbol{x}, 0) = \boldsymbol{\vartheta}_0(\boldsymbol{x}) \quad \text{in} \quad \Omega, \tag{5}$$

and the homogeneous Dirichlet boundary condition

$$\boldsymbol{\vartheta}(\boldsymbol{x}, t) = 0 \quad \text{on} \quad \Gamma_w \times (0, T), \tag{6}$$

where ρ is the constant flui density, p is the pressure, $-p\boldsymbol{I}$ is the spherical part of the stress due to the constraint of incompressibility, $\mu\big(|\dot{\gamma}|\big)$ is the shear-dependent viscosity function and

$$\boldsymbol{A}_1 = \nabla\boldsymbol{\vartheta} + \big(\nabla\boldsymbol{\vartheta}\big)^T \tag{7}$$

is the firs Rivlin-Ericksen tensor, $\nabla\boldsymbol{\vartheta}$ is the spatial velocity gradient and $\big(\nabla\boldsymbol{\vartheta}\big)^T$ is the transpose of $\nabla\boldsymbol{\vartheta}$. Equation $(4)_1$ represents the balance of linear momentum without body forces and $(4)_2$ is the incompressibility condition. In equation $(4)_3$, $\boldsymbol{T}$ is the constitutive equation associated a an generalized Newtonian flui and $\boldsymbol{t}_w$ denotes the stress vector on the surface whose outward unit normal vector is $\boldsymbol{\eta}(\boldsymbol{x}, t) = \eta_i(\boldsymbol{x}, t)\boldsymbol{e}_i$. The components of the outward unit normal vector to the surface of the vessel domain Ω are given by

$$\eta_1 = \frac{x_1}{\phi}, \quad \eta_2 = \frac{x_2}{\phi}, \quad \eta_3 = 0. \tag{8}$$

Concerning the shear-dependent viscosity function

$$\mu\big(|\dot{\gamma}|\big) : \mathbb{R}^+ \to \mathbb{R}^+,$$

$\dot{\gamma}$ is a scalar measure of the rate of shear define by $|\dot{\gamma}| = \sqrt{2\boldsymbol{D}:\boldsymbol{D}}$ with

$$\boldsymbol{D} := \frac{1}{2}\big(\nabla\boldsymbol{\vartheta} + \big(\nabla\boldsymbol{\vartheta}\big)^T\big)$$

being the rate of deformation tensor. The particular functional dependence on shear-rate is generally chosen in order to fi experimental data. In this work, we consider a power-law flui model, i.e.,

$$\mu(|\dot{\gamma}|) = k|\dot{\gamma}|^{n-1} \tag{9}$$

where the parameters k and n are positive constants called the consistency and the fl w index, respectively. If $n = 1$ in (9), the viscosity is a constant k

[3] In the general case when the scalar function ϕ depends on the spatial variable z and time t we have a fluid-structur interaction problem.

and blood is modeled as a Newtonian fluid If $n < 1$ at (9) then

$$\lim_{|\dot{\gamma}|\to+\infty} \mu(|\dot{\gamma}|) = 0, \quad \lim_{|\dot{\gamma}|\to 0} \mu(|\dot{\gamma}|) = +\infty,$$

and we have a shear-thinning flui behavior, i.e., the viscosity decreases monotonically with shear-rate. For $n > 1$ at (9), we get

$$\lim_{|\dot{\gamma}|\to+\infty} \mu(|\dot{\gamma}|) = +\infty, \quad \lim_{|\dot{\gamma}|\to 0} \mu(|\dot{\gamma}|) = 0,$$

and the flui shows a shear-thickening behavior, i.e., the viscosity increases with shear-rate. This theoretical model has limited applications to real fluid due to the unboundedness of the viscosity function, but is widely used and can be accurate for specifi fl w regimes. The theoretical study of the model $(4)-(6)$ with (9), namely existence, uniqueness and regularity of classical and weak solutions still poses some diffi culties. In this work we are interested in the numerical study of the model $(4)-(6)$ with (9), using the director approach related to flui dynamics. Since equation (3) define a material surface, the three-dimensional velocity fiel $\boldsymbol{\vartheta}$ must satisfy the kinematic condition[4]

$$\frac{d}{dt}\big(\phi^2 - x_1^2 - x_2^2\big) = 0$$

i.e.,

$$-x_1\vartheta_1 - x_2\vartheta_2 = 0 \tag{10}$$

on the boundary define by (3). Averaged quantities such as volume fl w rate and pressure are needed to study one-dimensional models. Consider $S = S(z,t)$ a generic axial section of the domain Ω at time t define by the spatial variable z, bounded by the circle define by (3), and let $A(z,t)$ be the area of this section $S(z,t)$. Then, the volume fl w rate Q is define by

$$Q(z,t) = \int_{S(z,t)} \vartheta_3(\boldsymbol{x},t)da, \tag{11}$$

and the average pressure $\bar{p}$, by

$$\bar{p}(z,t) = \frac{1}{A(z,t)} \int_{S(z,t)} p(\boldsymbol{x},t)da. \tag{12}$$

Starting with representation (1) it follows (see [10]) that the approximation of the three-dimensional velocity fiel $\boldsymbol{\vartheta} = \vartheta_i(\boldsymbol{x},t)\boldsymbol{e}_i$ using nine directors, is given by

$$\begin{aligned}\boldsymbol{\vartheta} = &\Big[x_1(\xi + \sigma(x_1^2+x_2^2)) - x_2(\omega + \eta(x_1^2+x_2^2))\Big]\boldsymbol{e}_1\\ &+ \Big[x_1(\omega + \eta(x_1^2+x_2^2)) + x_2(\xi + \sigma(x_1^2+x_2^2))\Big]\boldsymbol{e}_2\\ &+ \Big[v_3 + \gamma(x_1^2+x_2^2)\Big]\boldsymbol{e}_3,\end{aligned} \tag{13}$$

[4]The material time derivative is given by $\frac{d}{dt}(\,\cdot\,) = \frac{\partial}{\partial t}(\,\cdot\,) + \boldsymbol{\vartheta}\cdot\nabla(\,\cdot\,)$.

where $\xi, \omega, \gamma, \sigma, \eta$ are scalar functions of the spatial variable z and time t. The physical significanc of these scalar functions in (13) is the following: γ is related to tranverse shearing motion, ω and η are related to rotational motion (also called swirling motion) about $\boldsymbol{e}_3$, while ξ and σ are related to transverse elongation. We use nine directors because it is the minimum number for which the incompressibility condition and the kinematic boundary conditions on the lateral surface of the tube are satisfie pointwise. Using the velocity approach (13), the kinematic conditions (10) on the lateral boundary reduce to

$$-\phi^2(\xi + \phi^2\sigma) = 0 \tag{14}$$

and the incompressibility condition given by equation $(4)_2$ becomes

$$(v_3)_z + 2\xi + (x_1^2 + x_2^2)(\gamma_z + 4\sigma) = 0, \tag{15}$$

where the subscripted variable denotes partial differentiation. For equation (15) to hold at every point in the fluid the velocity coefficient must satisfy the separate conditions

$$(v_3)_z + 2\xi = 0, \quad \gamma_z + 4\sigma = 0. \tag{16}$$

Hence the boundary condition (10) and the incompressiblity condition given by equation $(4)_2$ are satisfie exactly by the velocity fiel (13) if we impose the conditions (14) and (16). On the wall boundary of the rigid tube we impose the no-slip boundary condition requiring that the velocity fiel (13) vanishes identically on the surface (3), i.e., condition (6) is satisfied Thus, it follows that

$$\xi + \phi^2\sigma = 0, \quad \omega + \phi^2\eta = 0, \quad v_3 + \phi^2\gamma = 0. \tag{17}$$

Therefore, equation (14) is satisfie identically and the two incompressiblity conditions (16) reduce to

$$(v_3)_z + 2\xi = 0, \quad (\phi^2 v_3)_z = 0. \tag{18}$$

Considering the fl w in a rigid tube with constant circular cross-section given by surface (3) without swirling motion (i.e., $\omega = \eta = 0$), conditions (11), (13), (17) and (18) then, the volume fl w rate Q is just a function of time t, given by

$$Q(t) = \frac{\pi}{2}\,\phi^2 v_3(z,t) \tag{19}$$

and, consequently, the velocity fiel (13) can be rewritten as

$$\boldsymbol{\vartheta}(\boldsymbol{x},t) = \frac{2Q(t)}{\pi\phi^2}\Big(1 - \frac{x_1^2+x_2^2}{\phi^2}\Big)\boldsymbol{e}_3, \tag{20}$$

and the initial condition (5) is satisfied when we consider in applications $Q(0) = cts$. To simplify our study, it is convenient to resolve the stress vector $\boldsymbol{t}_w$ on the lateral surface in terms of it is outward unit normal $\boldsymbol{\eta}$ and in terms of the components of the surface traction vector τ_1, τ_2 and p_e in the form

$$\boldsymbol{t}_w = \tau_1 \boldsymbol{\lambda} - p_e \boldsymbol{\eta} + \tau_2 \boldsymbol{e}_\theta, \tag{21}$$

where τ_1 is the wall shear stress, while $\boldsymbol{\lambda}$ and $\boldsymbol{e}_\theta$ are the unit tangent vectors define by

$$\boldsymbol{\lambda} = \boldsymbol{\eta} \times \boldsymbol{e}_\theta, \quad \boldsymbol{e}_\theta = (x_\alpha/\phi)\boldsymbol{e}_{\alpha\beta}\boldsymbol{e}_\beta, \tag{22}$$

with $\boldsymbol{e}_{11} = \boldsymbol{e}_{22} = 0$ and $\boldsymbol{e}_{12} = -\boldsymbol{e}_{21} = 1$ (see [10]). Using conditions (8) and (22), the expression for the stress vector (21) can be rewritten in terms of it is rectangular Cartesian components as

$$\boldsymbol{t}_w = \frac{1}{\phi}(-p_e x_1 - \tau_2 x_2)\boldsymbol{e}_1 + \frac{1}{\phi}(-p_e x_2 + \tau_2 x_1)\boldsymbol{e}_2 + \tau_1 \boldsymbol{e}_3. \tag{23}$$

Now, instead of the momentum equation $(4)_1$ be verifie pointwise in the fluid we impose the following integral conditions (see [10])

$$\int_S \Big[\nabla \cdot \boldsymbol{T} - \rho\Big(\frac{\partial \boldsymbol{\vartheta}}{\partial t} + \boldsymbol{\vartheta} \cdot \nabla \boldsymbol{\vartheta}\Big)\Big] da = 0, \tag{24}$$

$$\int_S \Big[\nabla \cdot \boldsymbol{T} - \rho\Big(\frac{\partial \boldsymbol{\vartheta}}{\partial t} + \boldsymbol{\vartheta} \cdot \nabla \boldsymbol{\vartheta}\Big)\Big] x_{\alpha_1} \dots x_{\alpha_N} da = 0, \tag{25}$$

where $N = 1, 2, 3$. Using the divergence theorem and a form of Liebnitz rule, equations (24) and (25) for nine directors, can be reduced to the following vector equations:

$$\frac{\partial \boldsymbol{n}}{\partial z} + \boldsymbol{f} = \boldsymbol{a} \tag{26}$$

and

$$\frac{\partial \boldsymbol{m}^{\alpha_1 \dots \alpha_N}}{\partial z} + \boldsymbol{l}^{\alpha_1 \dots \alpha_N} = \boldsymbol{k}^{\alpha_1 \dots \alpha_N} + \boldsymbol{b}^{\alpha_1 \dots \alpha_N}, \tag{27}$$

where $\boldsymbol{n}$, $\boldsymbol{k}^{\alpha_1 \dots \alpha_N}$, $\boldsymbol{m}^{\alpha_1 \dots \alpha_N}$ are resultant forces define by

$$\boldsymbol{n} = \int_S \boldsymbol{T}_3 da, \quad \boldsymbol{k}^\alpha = \int_S \boldsymbol{T}_\alpha da, \tag{28}$$

$$\boldsymbol{k}^{\alpha\beta} = \int_S \Big(\boldsymbol{T}_\alpha x_\beta + \boldsymbol{T}_\beta x_\alpha\Big) da, \tag{29}$$

$$\boldsymbol{k}^{\alpha\beta\gamma} = \int_S \Big(\boldsymbol{T}_\alpha x_\beta x_\gamma + \boldsymbol{T}_\beta x_\alpha x_\gamma + \boldsymbol{T}_\gamma x_\alpha x_\beta\Big) da \tag{30}$$

and

$$\boldsymbol{m}^{\alpha_1 \dots \alpha_N} = \int_S \boldsymbol{T}_3 x_{\alpha_1} \dots x_{\alpha_N} da. \tag{31}$$

The quantities $\boldsymbol{a}$ and $\boldsymbol{b}^{\alpha_1 \dots \alpha_N}$ are inertia terms define by

$$\boldsymbol{a} = \int_S \rho\Big(\frac{\partial \boldsymbol{\vartheta}}{\partial t} + \boldsymbol{\vartheta} \cdot \nabla \boldsymbol{\vartheta}\Big) da, \tag{32}$$

$$\boldsymbol{b}^{\alpha_1 \dots \alpha_N} = \int_S \rho\Big(\frac{\partial \boldsymbol{\vartheta}}{\partial t} + \boldsymbol{\vartheta} \cdot \nabla \boldsymbol{\vartheta}\Big) x_{\alpha_1} \dots x_{\alpha_N} da \tag{33}$$

and $\boldsymbol{f}$, $\boldsymbol{l}^{\alpha_1 \dots \alpha_N}$, which arise due to surface traction on the lateral boundary, are define by

$$\boldsymbol{f} = \int_{\partial S} \boldsymbol{t}_w \, ds, \tag{34}$$

$$\boldsymbol{l}^{\alpha_1 \dots \alpha_N} = \int_{\partial S} \boldsymbol{t}_w \, x_{\alpha_1} \dots x_{\alpha_N} ds. \tag{35}$$

The equation for the mean pressure gradient will be obtained using the resulting quantities from (28) to (35) on equations (26) – (27). On equations (34) – (35) we will apply the stress vector $\boldsymbol{t}_w$ given by (23). Now, using the velocity fiel (20), the surface (3), the volume fl w rate (19), the incompressiblity contrains (16), no-slip conditions $(17)_{1,3}$ and the stress vector (23) in equations (28) to (35), we can explicitly calculate the forces $\boldsymbol{n}$, $\boldsymbol{k}^{\alpha_1 \dots \alpha_N}$, $\boldsymbol{m}^{\alpha_1 \dots \alpha_N}$, the inertia terms $\boldsymbol{a}$, $\boldsymbol{b}^{\alpha_1 \dots \alpha_N}$ and the surface tractions $\boldsymbol{f}$, $\boldsymbol{l}^{\alpha_1 \dots \alpha_N}$. Hence, plugging these solutions into equations (26) – (27) and using equation (12), we get by solving a linear system the unsteady equation for the average pressure gradient, given by

$$\bar{p}_z(z,t) = -\frac{4\rho Q_t(t)}{3\pi\phi^2} - \frac{4k\big(2^{\frac{5n+1}{2}}\big)Q^n(t)}{(n+3)\pi^n\phi^{3n+1}}. \tag{36}$$

Integrating equation (36), over a finit section of the tube with $z_1 < z_2$, we get the mean pressure gradient over the interval $[z_1, z_2]$ at time t, given by

$$G(t) = \frac{\bar{p}(z_1,t) - \bar{p}(z_2,t)}{z_2 - z_1} = \frac{4\rho Q_t(t)}{3\pi\phi^2} + \frac{4k\big(2^{\frac{5n+1}{2}}\big)Q^n(t)}{(n+3)\pi^n\phi^{3n+1}}. \tag{37}$$

Now, let us consider the following dimensionless variables

$$\hat{t} = \omega_0 t, \quad \hat{Q} = \frac{2\rho}{\pi\phi k} Q, \quad \hat{G} = \frac{\rho^n \phi^{2n+1}}{k^{n+1}} G, \tag{38}$$

where ω_0 is the characteristic frequency for unsteady fl ws. In the cases where a steady volume fl w rate is specified the nondimensional volume fl w rate $\hat{Q}$ is identical to the classical $\mathcal{R}_e$ (Reynolds number) used for fl w in tubes. Substituting the new variables (38) in equation (37), we obtain the nondimensional mean pressure gradient

$$\hat{G}(\hat{t}) = \frac{2}{3}\mathcal{W}_o^2 \hat{Q}_{\hat{t}}(\hat{t}) + \frac{2^{\frac{3n+5}{2}}}{n+3}\hat{Q}^n(\hat{t}), \qquad (39)$$

where $\mathcal{W}_o = \phi^n\sqrt{\rho^n\omega_0/k^n}$ is the Womersley number, which is the most commonly used parameter to reflec the pulsatility of the fl w. Using $(38)_2$ and

$$\hat{x}_1 = \frac{x_1}{\phi}, \quad \hat{x}_2 = \frac{x_2}{\phi}, \quad \hat{z} = \frac{z}{\phi}, \quad \hat{\boldsymbol{\vartheta}} = \frac{\phi\rho}{k}\boldsymbol{\vartheta} \qquad (40)$$

at the velocity equation (20), we get the nondimensional three-dimensional velocity fiel

$$\hat{\boldsymbol{\vartheta}}(\hat{\boldsymbol{x}}, \hat{t}) = \hat{Q}(\hat{t})\Big(1 - (\hat{x}_1^2 + \hat{x}_2^2)\Big)\boldsymbol{e}_3. \qquad (41)$$

From equation (39), the volume fl w rate in the steady case is given by

$$\hat{Q} = \sqrt[n]{\frac{n+3}{2^{\frac{3n+5}{2}}}\hat{G}}. \qquad (42)$$

In order to evaluate the fl w predictions of the one-dimensional theory developed here, we next consider the exact three-dimensional volume fl w rate of an axisymmetric steady fl w through a straight tube with constant circular cross-section, given by (see Bird et al. [15])

$$\tilde{Q} = \frac{n}{3n+1}\sqrt[n]{2^{n-1}\hat{G}}. \qquad (43)$$

Next, we present numerical simulations associated with equations (39), (41), (42) and (43) for specifi fl w regimes.

3 Numerical results

In this session we will present numerical results associated to equation (39) where the mean pressure gradient will be given and we will check the evolution of the volume fl w rate for specifi fl w regimes. Consequently, we present the behavior of the three-dimensional velocity fiel (41) in the circular cross-section of the tube. Finally, considering the steady case, we will compare the exact solution (43) with the approximate solution (42), validating in this way and for specifi data the Cosserat theory as a valid alternative for the three-dimensional study of a specifi physical model associated to the fl w of a fluid

3.1 Steady problem

In the steady case, let us compare the exact volume fl w rate solution (43) with the volume fl w rate approximate solution (42). In Figure 2, we can see the steady volume fl w rate (42) behavior for a fi ed value of the mean pressure gradient as a function of the fl w index, concluding that the solution converges to a certain value as we increase the fl w index for a given mean pressure gradient. Comparing the ap-

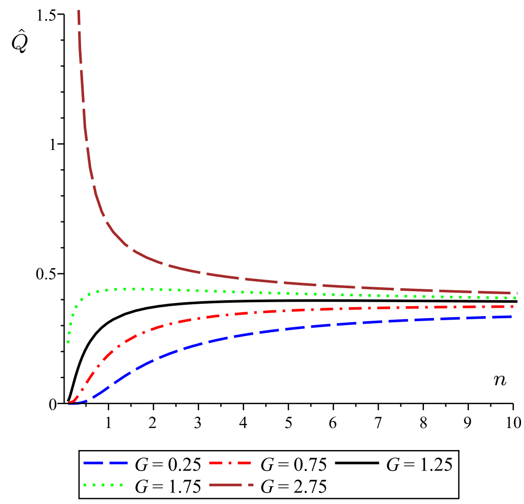

Figure 2: Variation of the steady volume fl w rate (42) as a function of fl w index with fi ed mean pressure gradient.

proximate solution for volume fl w rate with the exact solution we can conclude that the approximation is excellent for the case of shear-thinning fluid which is the relevant case in this work, see Figure 3. Considering this comparation, we can state that in this case the Cosserat theory is valid for fl w index values such that $0 << n < 1$ with small range of mean pressure gradient, the situation $n \to 0$ is neglected because it has no physical meaning in this work. In the case of shear-thickening fluid the comparison is no longer relevant as the fl w index increases, see Figure 3. Also, we can conclude that the approximation solution (42) is not relevant when we increase the mean pressure gradient, see Figure 3 and Figure 4. For blood fl w the range of the mean pressure gradient is very small.

Next, we will illustrate the behavior of the three-dimensional steady velocity fiel (41) where the steady volume fl w rate (42) is given with $\hat{G}$ and fl w index fi ed. In the case of $\hat{G} = 1.75$, Figure 5 and Figure 6 shown us very small variation on the intensity of the steady velocity (41) for shear-thinning flui and shear-thickening fluid respectively. Next, we consider the behavior of the steady velocity (41) when we increase the constant mean pressure gradient

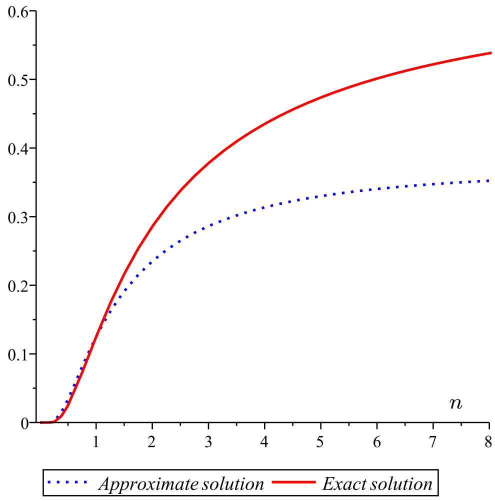

Figure 3: Comparison between the exact solution (43) and the approximate solution (42) for the steady volume fl w rate as a function of fl w index with small mean pressure gradient $\hat{G} = 0.5$.

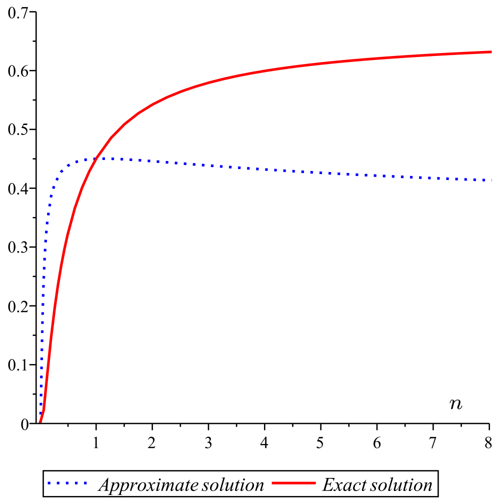

Figure 4: Comparison between the exact solution (43) and the approximate solution (42) for the steady volume fl w rate as a function of fl w index with mean pressure gradient $\hat{G} = 1.8$.

$\hat{G} = 2.75$, see Figure 7 and Figure 8. This results are in excellent agreement with the behavior of the steady volume fl w rate shown in Figure 2.

3.2 Unsteady problem

In Figure 9, we can observe the behavior of the unsteady volume fl w rate solution given by (39) obtained using a Runge-Kutta method with constant mean pressure gradient $\hat{G}(\hat{t}) = \hat{G} = 1$ in the case of

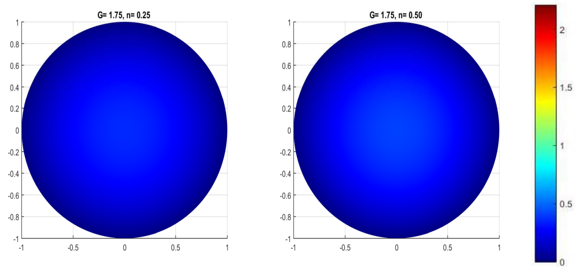

(a) $\mathcal{R}_e \simeq 0.36$ (b) $\mathcal{R}_e \simeq 0.41$

Figure 5: Three-dimensional steady velocity fiel (41) with steady volume fl w rate (42), where $\mathcal{R}_e \simeq 0.36$ ($\hat{G} = 1.75, n = 0.25$) and $\mathcal{R}_e \simeq 0.41$ ($\hat{G} = 1.75, n = 0.5$)

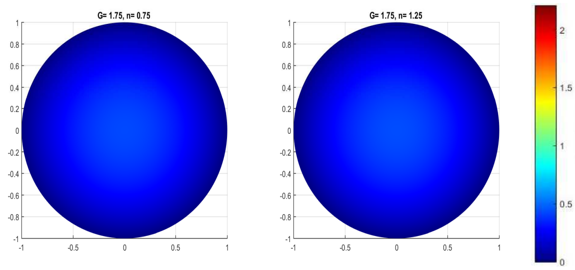

(a) $\mathcal{R}_e \simeq 0.43$ (b) $\mathcal{R}_e \simeq 0.44$

Figure 6: Three-dimensional steady velocity fiel (41) with steady volume fl w rate (42), where $\mathcal{R}_e \simeq 0.43$ ($\hat{G} = 1.75, n = 0.75$) and $\mathcal{R}_e \simeq 0.44$ ($\hat{G} = 1.75, n = 1.25$).

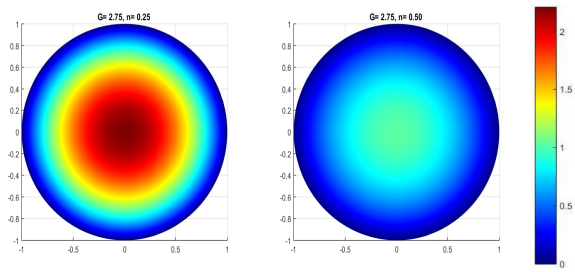

(a) $\mathcal{R}_e \simeq 2.20$ (b) $\mathcal{R}_e \simeq 1.02$

Figure 7: Three-dimensional steady velocity fiel (41) with steady volume fl w rate (42), where $\mathcal{R}_e \simeq 2.20$ ($\hat{G} = 2.75, n = 0.25$) and $\mathcal{R}_e \simeq 1.02$ ($\hat{G} = 2.75, n = 0.5$)

shear-thinning flui when we increase the Womersley number. We note that while the fl w index n increases the amplitude of the solution in the initial transient phase increases and becomes less pronounced as the Womersley number increases. In this particular case of a constant mean pressure gradient, the system (39) converges toward a steady state solution. When we

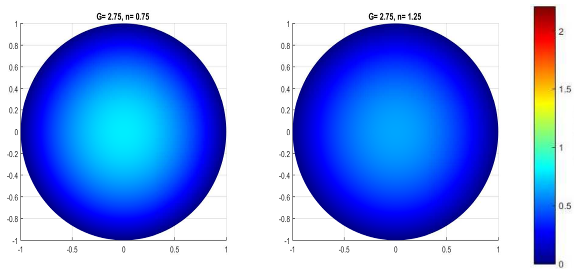

(a) $\mathcal{R}_e \simeq 0.78$ (b) $\mathcal{R}_e \simeq 0.63$

Figure 8: Three-dimensional steady velocity fiel (41) with steady volume fl w rate (42), where $\mathcal{R}_e \simeq 0.78$ ($\hat{G} = 2.75, n = 0.75$) and $\mathcal{R}_e \simeq 0.63$ ($\hat{G} = 2.75, n = 1.25$).

move from a situation of shear-thinning flui to shear-thickening fluid the behavior of the volume fl w rate solution is similar, i.e., as we increase the fl w index the amplitude of the solution in the initial transient phase increases, see Figure 10. Consequently, we can see that the behavior of the volume fl w rate solution is similar for shear-thinning flui and shear-thickening fluid respectively. But, in the case shear-thinning flui the volume fl w rate solution presents amplitudes of lower value in comparison with the case of a shear-thickening fluid such situation may be relevant in certain physical applications. Now, with the information of the volume fl w rate (39) obtained for certain fl w regimes we can return to the three-dimensional situation to obtain the behavior of the velocity fiel (41) in time in the circular cross-section of the tube.

The Figure 11 and Figure 12, illustrate the three-dimensional velocity fiel (41) behavior in the circular cross-section of the tube in the initial transition phase, and we can see the increase of the velocity intensity as we increase the fl w index in a situation of shear-thinning fluid Also, we can see that the velocity field needs a very short time to stabilize at a constant intensity, and this is due to the initial transition phase. In our study, the shear-thinning flui situation is taken into account for blood fl w. In the case of shear-thickening fluid see Figure 13 and Figure 14, we can verify that the increase of the fl w index from shear-thinning flui to the shear-thickening flui increases the velocity fiel intensity for the same initial transition phase with the same fl w regimes. Next, we consider non-constant mean pressure gradient, given by equation (44)

$$\hat{G}(\hat{t}) = 1 + \frac{\sin^2(\hat{t})}{e^{\hat{t}}}, \tag{44}$$

which shows an interesting behavior, see Figure 15. More specificall it shows a strong variation in the

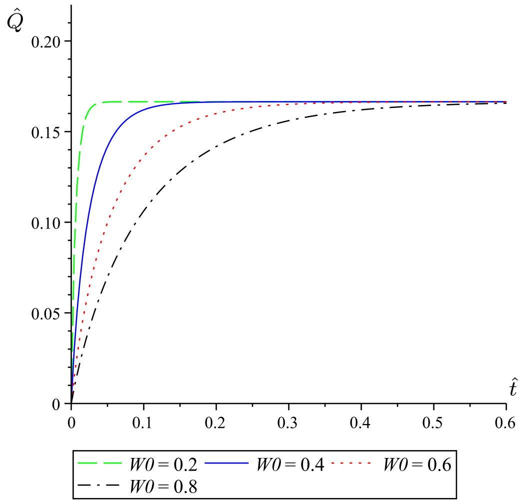

(a) Flow index $n = 0.6$.

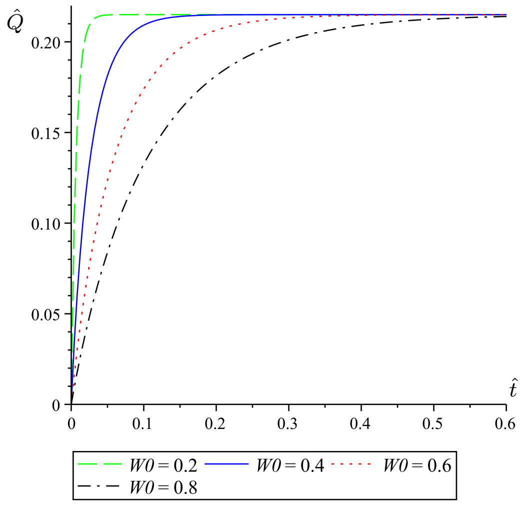

(b) Flow index $n = 0.8$.

Figure 9: Unsteady volume fl w rate (39) with constant mean pressure gradient $\hat{G}(\hat{t}) = \hat{G} = 1$ where $\hat{Q}(0) = 0$, $\mathcal{W}_o = (0.2, 0.4, 0.6, 0.8)$ for shear-thinning fluid

initial stage and after the initial transient phase has small fluctuations which tend to decrease with time. Considering the mean pressure gradient (44) on equation (39) and using a Runge-Kutta method for specifi fl w regimes we can get information about the volume fl w rate behavior. Shown in Figure 16, results for volume fl w rate in the case of shear-thinning flui and we can see the amplitude of the volume fl w rate increase with the fl w index in the initial transition phase, which tends to follow the behavior of the mean pressure gradient function (44), the fluctuation in the solution decreases in time.

Figure 17, shows us that in the initial transition

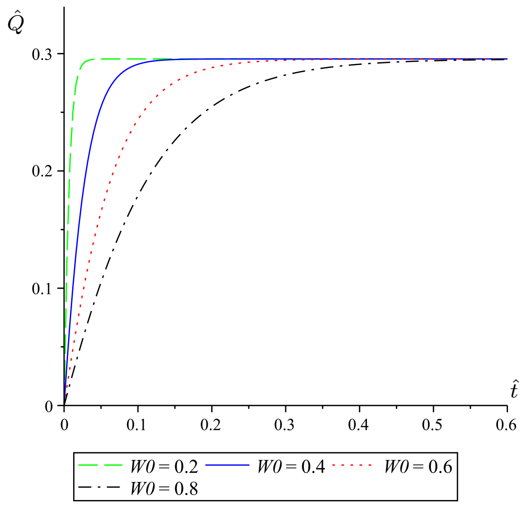

(a) Flow index $n = 1.4$.

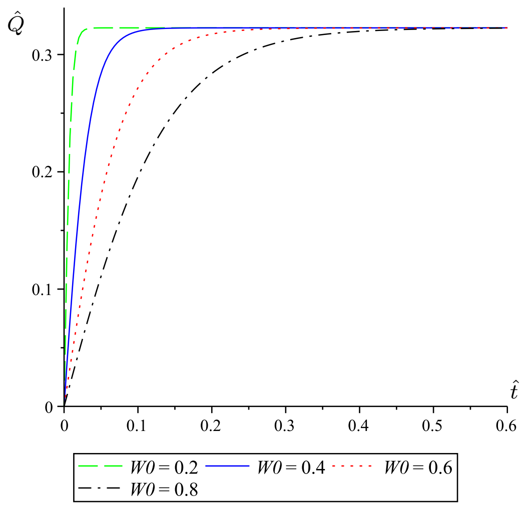

(b) Flow index $n = 1.8$.

Figure 10: Unsteady volume fl w rate (39) with constant mean pressure gradient $\hat{G}(\hat{t}) = \hat{G} = 1$ where $\hat{Q}(0) = 0$, $\mathcal{W}_o = (0.2, 0.4, 0.6, 0.8)$ for shear-thickening fluid

phase the amplitude of the volume fl w rate tries to increase with the increase of the fl w index. Therefore, Figure 16 and Figure 17 shows us the evolution of the volume fl w rate as we move from a shear-thinning flui situation to a shear-thickening flui situation. Next, we will see the behavior of the three-dimensional velocity field

The Figure 18 and Figure 19, shows us the three-dimensional velocity fiel (41) intensity for specifi fl w regimes in the case of shear-thinning flui during the initial transition phase. In comparison with the constant mean pressure gradient case, we can see that in this case where the mean pressure gradient is non-constant, the velocity fiel intensity increases during the initial transition phase. The same conclusions for the case of shear-thickening fluid see Figure 20 and Figure 21.

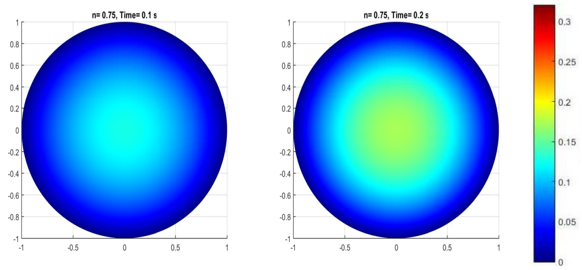

Figure 11: Three-dimensional velocity fiel (41) where the volume fl w rate is obtained by (39) with mean pressure gradient $\hat{G}(\hat{t}) = \hat{G} = 1$, $\hat{Q}(0) = 0$, $\mathcal{W}_o = 0.8$ and $n = 0.75$ (shear-thinning fluid) Time parameters: $\hat{t} = 0.1, \hat{t} = 0.2$.

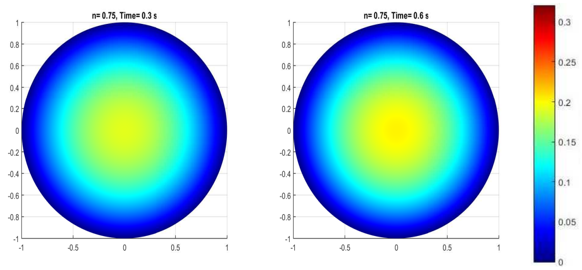

Figure 12: Three-dimensional velocity fiel (41) where the volume fl w rate is obtained by (39) with mean pressure gradient $\hat{G}(\hat{t}) = \hat{G} = 1$, $\hat{Q}(0) = 0$, $\mathcal{W}_o = 0.8$ and $n = 0.75$ (shear-thinning fluid) Time parameters: $\hat{t} = 0.3, \hat{t} = 0.6$.

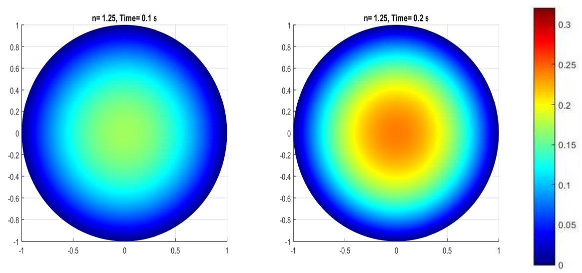

Figure 13: Three-dimensional velocity fiel (41) where the volume fl w rate is obtained by (39) with mean pressure gradient $\hat{G}(\hat{t}) = \hat{G} = 1$, $\hat{Q}(0) = 0$, $\mathcal{W}_o = 0.8$ and $n = 1.25$ (shear-thickening fluid) Time parameters: $\hat{t} = 0.1, \hat{t} = 0.2$.

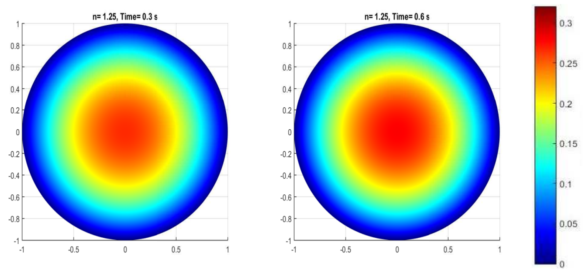

Figure 14: Three-dimensional velocity fiel (41) where the volume fl w rate is obtained by (39) with mean pressure gradient $\hat{G}(\hat{t}) = \hat{G} = 1$, $\hat{Q}(0) = 0$, $\mathcal{W}_o = 0.8$ and $n = 1.25$ (shear-thickening fluid) Time parameters: $\hat{t} = 0.3, \hat{t} = 0.6$.

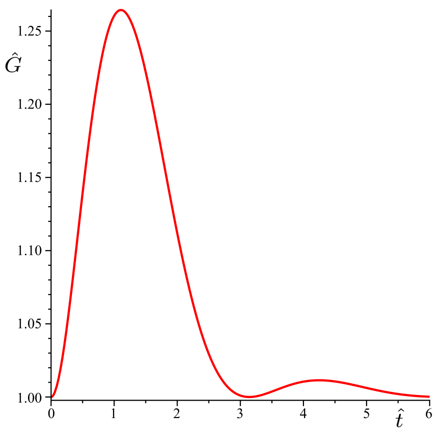

Figure 15: Non-constant mean pressure gradient given by (44).

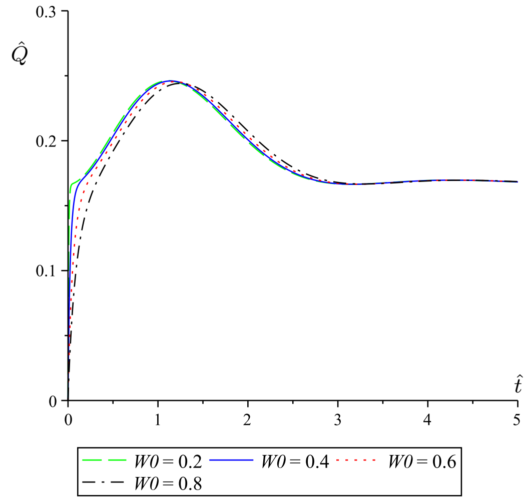

(a) Flow index $n = 0.6$.

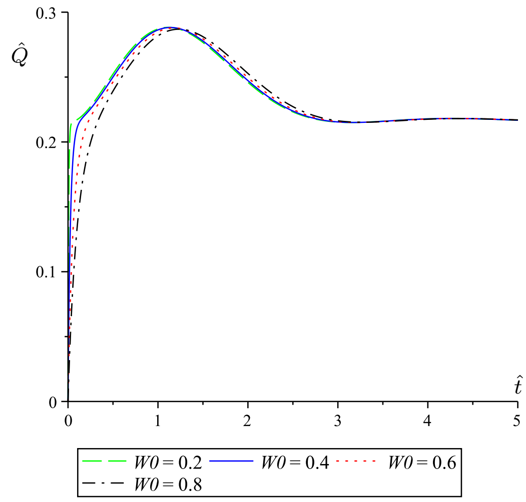

(b) Flow index $n = 0.8$.

Figure 16: Unsteady volume fl w rate (39) with non-constant mean pressure gradient (44) where $\hat{Q}(0) = 0$ and $\mathcal{W}_o = (0.2, 0.4, 0.6, 0.8)$ for shear-thinning fluid

4 Perturbations flows

In many physical applications involving flui fl ws in specifi domains it is important to determine the changes in fl w characteristics induced by perturbations in the initial or boundary data, body forces or pressure drop. In fact, since it is virtually impossible to maintain an exactly constant pressure drop, one should be able to predict how much a perturbation of given magnitude in pressure drop will affect the volume fl w rate. Therefore, let us consider a uniform perturbation of magnitude ε at the function (44) (see Figure 22). For each $\varepsilon > 0$, definin the quantities,

$$\hat{G}^+_\varepsilon(\hat{t}) = (1+\varepsilon)\hat{G}(\hat{t}), \quad \hat{G}^-_\varepsilon(\hat{t}) = (1-\varepsilon)\hat{G}(\hat{t}), \tag{45}$$

we denote by $\hat{Q}^+_\varepsilon$ and $\hat{Q}^-_\varepsilon$ the perturbed volume fl w rates corresponding to $\hat{G}^+_\varepsilon$ and $\hat{G}^-_\varepsilon$, respectively. Next, we will consider a perturbation in the approximate solution obtained by the Cosserat theory and we will verify the stability of the one-dimensional solution.

4.1 Steady problem

Considering the perturbation

$$\hat{G}^\pm_\varepsilon = (1 \pm \varepsilon)\hat{G},$$

where $\hat{G}$ is a constant mean pressure gradient, for sufficientl large $\hat{t}$, after the initial transient phase, we can use the characterization of the steady solution deduced in (42), and explicitly compute the perturbed

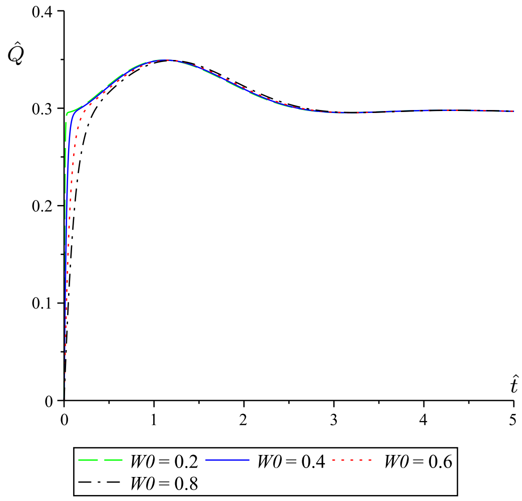

(a) Flow index $n = 1.4$.

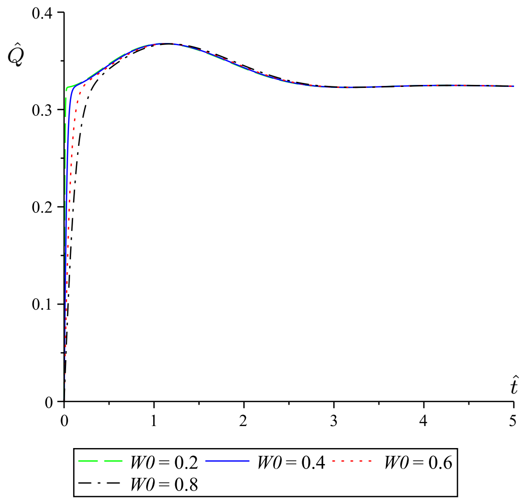

(b) Flow index $n = 1.8$.

Figure 17: Unsteady volume fl w rate (39) with non-constant mean pressure gradient (44) where $\hat{Q}(0) = 0$ and $\mathcal{W}_o = (0.2, 0.4, 0.6, 0.8)$ for shear-thickening fluid

volume fl w rate, using (45), as follows:

$$\hat{Q}_\varepsilon^\pm = \sqrt[n]{\frac{n+3}{2^{\frac{3n+5}{2}}}\hat{G}_\varepsilon^\pm} = \sqrt[n]{\frac{n+3}{2^{\frac{3n+5}{2}}}(1\pm\varepsilon)\hat{G}}$$
$$= \sqrt[n]{\frac{n+3}{2^{\frac{3n+5}{2}}}\hat{G}}(1\pm\varepsilon)^{1/n}$$
$$= \hat{Q}(1\pm\varepsilon)^{1/n}. \qquad (46)$$

Normalizing the above perturbeded volume fl w rate $\hat{Q}_\varepsilon^\pm$ by the unperturbed volume fl w rate $\hat{Q}$, we get

$$\frac{\hat{Q}_\varepsilon^\pm}{\hat{Q}} = (1\pm\varepsilon)^{1/n}, \qquad (47)$$

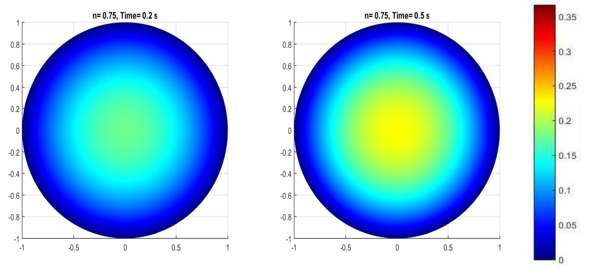

Figure 18: Three-dimensional velocity fiel (41) where the volume fl w rate is obtained by (39) with mean pressure gradient (44), $\hat{Q}(0) = 0$, $\mathcal{W}_o = 0.8$ and $n = 0.75$ (shear-thinning fluid) Time parameters: $\hat{t} = 0.2, \hat{t} = 0.5$.

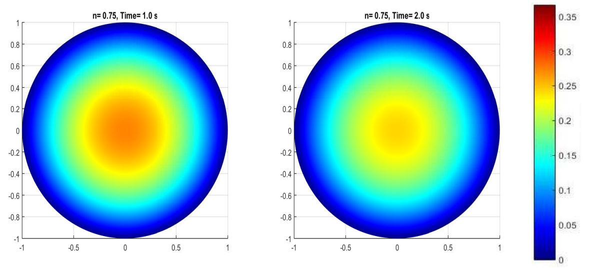

Figure 19: Three-dimensional velocity fiel (41) where the volume fl w rate is obtained by (39) with mean pressure gradient (44), $\hat{Q}(0) = 0$, $\mathcal{W}_o = 0.8$ and $n = 0.75$ (shear-thinning fluid) Time parameters: $\hat{t} = 1, \hat{t} = 2$.

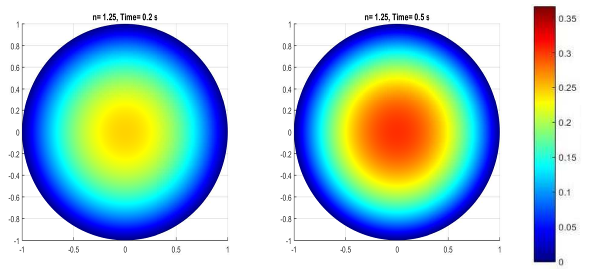

Figure 20: Three-dimensional velocity fiel (41) where the volume fl w rate is obtained by (39) with mean pressure gradient (44), $\hat{Q}(0) = 0$, $\mathcal{W}_o = 0.8$ and $n = 1.25$ (shear-thickening fluid) Time parameters: $\hat{t} = 0.2, \hat{t} = 0.5$.

which means that in the steady case, this kind of multiplicative perturbation acts linearly. Changing the mean pressure gradient by a factor of $(1 \pm \varepsilon)$, we changes the unperturbed volume fl w rate by a factor of $(1 \pm \varepsilon)^{1/n}$. In particular this shows that the steady state solution is linearly stable. Perturbations will be negligible if $(1 \pm \varepsilon)^{1/n} \simeq 1$, which happens when $\varepsilon \to 0$ (i.e., for small changes in the mean pres-

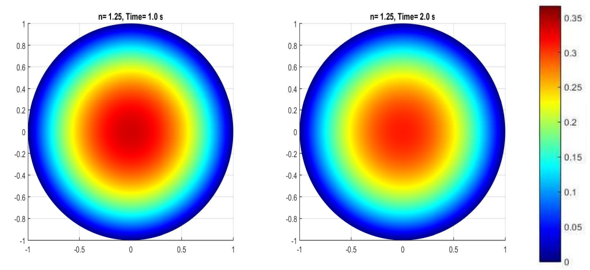

Figure 21: Three-dimensional velocity fiel (41) where the volume fl w rate is obtained by (39) with mean pressure gradient (44), $\hat{Q}(0) = 0$, $\mathcal{W}_o = 0.8$ and $n = 1.25$ (shear-thickening fluid) Time parameters: $\hat{t} = 1, \hat{t} = 2$.

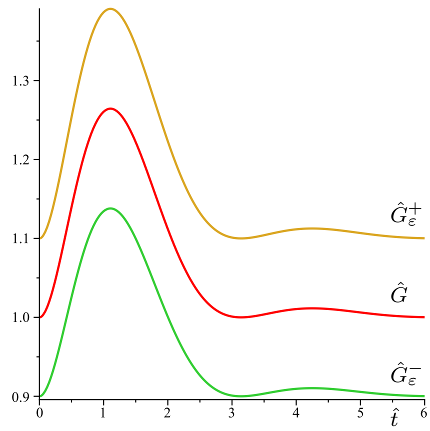

Figure 22: Multiplicative perturbation of the mean pressure gradient (44), with magnitude $\varepsilon = 0.1$.

sure gradient) or when the fl w index related with the viscosity goes to infinit , i.e., shear-thickening fluid with high fl w index.

4.2 Unsteady problem

In the case of non-constant mean pressure gradient the same ideas hold, apart from the fact that it is no longer possible to deduce exact expressions for the perturbed volume fl w rates. However, we can compute the time evolution of the perturbation volume fl w rate $\hat{Q}_\varepsilon^\pm$. In Figure 23, we illustrate the time evolution of the volume fl w rate with mean pressure gradient (44), together with the perturbed fl w rates $\hat{Q}_\varepsilon^\pm$ of magnitude $\varepsilon = 0.1$, forming a strip around $\hat{Q}$ containing all perturbations of magnitude less or equal to ε. Figure 24, shows the amplitude of this strip

$$|\hat{Q}_\varepsilon^+ - \hat{Q}_\varepsilon^-| \tag{48}$$

for several values of fl w index n with fi ed Womersley number, showing that increasing the fl w index

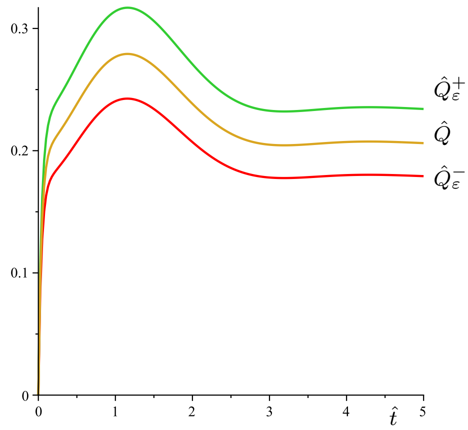

(a) Flow index $n = 0.75$.

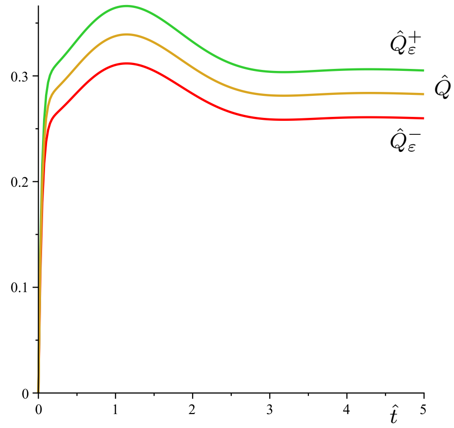

(b) Flow index $n = 1.25$.

Figure 23: Time evolution of the unperturbed volume fl w rate $\hat{Q}$, and perturbed volume fl w rate $\hat{Q}_\varepsilon^\pm$, with magnitude $\varepsilon = 0.1$ and $\mathcal{W}_o = 0.5$ for shear-thinning and shear-thickening fluids respectively.

n reduces sensitivity to the perturbations, as already mentioned in the case of a constant mean pressure gradient.

5 Conclusion

In this work, the Cosserat theory has been used to derive a one-dimensional power-law flui model in a straight, rigid and impermeable tube with uniform circular cross-section, as an alternative approach, to predict some of the main properties of associated three-dimensional models. Unsteady nondimensional equation for the mean pressure gradient depending on the volume fl w rate, Womersley number and the fl w index over a finit section of the tube geometry has been obtained. Taking into account the volume fl w rate approximate solution for certain fl w regimes we obtained relevant information about the

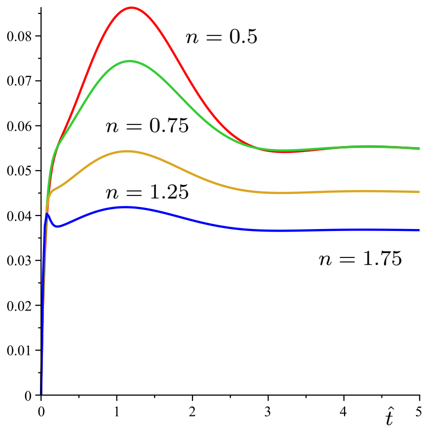

Figure 24: Time evolution of perturbation (48) for different values of fl w index ($n = 0.5, n = 0.75, n = 1.25, n = 1.75$), with $\mathcal{W}_o = 0.5$ and magnitude $\varepsilon = 0.1$.

behavior of the intensity of the three-dimensional velocity fiel in the circular cross-section of the tube. The predictive capability of this approach theory to study the unsteady fl w behavior has been evaluated by comparing its one-dimensional solution with the three-dimensional exact solution for steady fl ws. We have a good match of the results for shear-thinning flui situation, which is related to the study of blood fl w in the human circulatory system. This theory has strong limitations for sufficientl low and/or high fl w index n to real fluid due to the unboundedness of the viscosity asymptotic limits, but can be widely used and accurate for specifi fl w regimes. Also, we conducted numerical results for perturbed fl ws, obtaining an exact expression for the perturbed volume fl w rates in the steady case, providing a firs step towards stability analysis of the model. One of the possible extensions of this work is the application of this one-dimensional approach theory to study the same power-law fl w model in curved tubes, fluid-structur interaction and tubes with branches or bifurcations.

Acknowledgements: This work has been partially supported by Centro de Investigação em Matemática e Aplicações da Universidade de Évora (CIMA-UE), Portugal, through the grant UID/MAT/04674/2013 of FCT-Fundação para a Ciência e a Tecnologia. The author, Ricardo Conceição acknowledge the Institute of Earth Sciences, University of Évora (IES-UE) and also FCT because the scholarship SFRH/BD/116344/2016.

References:

[1] W. Harvey, *Exercitatio anatomica de motu cordis et sanguinis in animalibus*, Frankfurt, W. Fitzeri, 1628.

[2] S. Chien, S. Usami, R.J. Delenback and M.L. Gregersen, Blood Viscosity: Influenc of erythrocyte deformation, *Science* 157(3790), 1967, pp. 827–829.

[3] S. Chien, S. Usami, R.J. Delenback and M.L. Gregersen, Blood Viscosity: Influenc of erythrocyte aggregation, *Science* 157(3790), 1967, pp. 829–831.

[4] G.B. Thurston, Viscoelasticity of human blood, *Biophys. J.* 12, 1972, pp. 1205–1217.

[5] O.K. Baskurt and H.J. Meiselman, Blood rheology and hemodynamics, *Seminars in Trombosis and Hemostasis* 29, 2003, pp. 435–450.

[6] L. Euler, Principia pro motu sanguinis per arterias determinando, *Opera poshuma mathematica et physica anno 1844 detecta* 2, 1775, pp. 814–823.

[7] T. Hughes and J. Lubliner, On the one-dimensional theory of blood fl w in the larger vessels, *Mathematical Biosciences* 18, 1973, pp. 161–170.

[8] S.J. Sherwin, V. Franke, J. Peiró and K. Parker, One-dimensional modelling of a vascular network in space-time variables, *Journal of Engineering Mathematics* 47, 2003, pp. 217–250.

[9] L. Formaggia, D. Lampont and A. Quarteroni, One-dimensional models for blood fl w in arteries, *Journal of Engineering Mathematics* 47, 2003, pp. 251–276.

[10] D.A. Caulk and P.M. Naghdi, Axisymmetric motion of a viscous flui inside a slender surface of revolution, *Journal of Applied Mechanics* 54, 1987, pp. 190–196.

[11] A.E. Green and P.M. Naghdi, A direct theory of viscous flui fl w in pipes I: Basic general developments, *Phil. Trans. R. Soc. Lond. A* 342(1), 1993, pp. 525–542.

[12] A.E. Green, P.M. Naghdi and M.J. Stallard, A direct theory of viscous flui fl w in pipes II: Flow of incompressible viscous flui in curved pipes, *Phil. Trans. R. Soc. Lond. A* 342(1), 1993, pp. 543–572.

[13] A.M. Robertson and A. Sequeira, A director theory approach for modeling blood fl w in the arterial system: an alternative to classical 1d models, *Math. Models Methods Appl. Sci.* 15(6), 2005, pp. 871–906.

[14] F. Carapau and A. Sequeira, 1D Models for Blood Flow in Small Vessels Using the Cosserat Theory, *WSEAS Transactions on Mathematics* 5(1), 2006, pp. 54–62.

[15] B.R. Bird, R.C. Armstrong and O. Hassager, *Dynamics of Polymeric Liquids*, Vol. 1, 2nd edition, John Wiley & Sons, 1987.